Int. J. Heat Mass Transfer. Vol. 17, pp. 835–843. Pergamon Press 1974. Printed in Great Britain

NATURAL CONVECTION EFFECTS ON GRAETZ PROBLEM IN HORIZONTAL RECTANGULAR CHANNELS WITH UNIFORM WALL TEMPERATURE FOR LARGE *Pr*

JENN-WUU OU, K. C. CHENG and RAN-CHAU LIN
Department of Mechanical Engineering, University of Alberta, Edmonton, Alberta, Canada

(*Received* 21 *May* 1973 *and in revised form* 19 *November* 1973)

Abstract—The effect of buoyancy forces on laminar forced convective heat transfer in the thermal entrance region of horizontal rectangular channels with uniform wall temperature is studied by a numerical method for the case of large Prandtl number fluids. The numerical results are presented for the aspect ratios (width/height) 0·5, 1, 2 and Rayleigh numbers $0 \sim 5 \times 10^5$. The correlation equations for the prediction on the onset of significant free convection effect are developed. The asymptotic behavior of local Nusselt number is compared against the known asymptote for the uniform wall temperature boundary condition. The entrance region where the free convection effect is significant is clearly established and the classical Graetz problem is shown to be a limiting case and is applicable only when $Ra \leqslant 10^3$.

NOMENCLATURE

A,	cross-sectional area of a rectangular channel;
a, b,	width and height of a channel, respectively;
C,	a constant, $(D_e^2/\mu \overline{W}_f)\partial P_f/\partial Z$;
D_e,	equivalent hydraulic diameter, $4A/S$;
Gr,	Grashof number, $g\beta\theta_c D_e^3/\nu^2$;
g,	gravitational acceleration;
$\bar{h}$,	average heat-transfer coefficient;
k,	thermal conductivity;
M, N,	number of divisions in X and Y directions, respectively;
Nu,	local Nusselt number, $\bar{h}D_e/k$;
n,	dimensionless outward normal distance to the wall based on D_e;
Pr,	Prandtl number, ν/κ;
Ra,	Rayleigh number, $PrGr$;
Re,	Reynolds number, $\overline{W}_f D_e/\nu$;
S,	circumference of cross-section;
T,	liquid temperature;
T_0, T_w,	uniform entrance temperature and constant wall temperature, respectively;
U, V, W,	velocity components in X, Y, Z, directions due to buoyancy effect;
u, v, w,	dimensionless quantities for U, V and W;
W_f,	fully developed axial velocity before thermal entrance;
w_f,	dimensionless quantity for W_f;
X, Y, Z,	rectangular co-ordinates;
x, y, z,	dimensionless rectangular co-ordinates.

Greek letters

β,	coefficient of thermal expansion;
γ,	aspect ratio of a rectangular channel, a/b;
θ, θ_c,	dimensionless temperature difference, $(T - T_w)/\theta_c$ and characteristic temperature difference, $(T_0 - T_w)$, respectively;
κ,	thermal diffusivity;
μ,	viscosity;
ν,	kinematic viscosity;
ξ,	vorticity, $\nabla^2\psi$;
ρ,	density;
ψ,	dimensionless stream function.

Subscripts

b,	bulk temperature;
w,	value at wall.

Superscript

$-$,	average value.

1. INTRODUCTION

THE EXISTING theoretical methods of analysis for laminar convective heat transfer in the thermal entrance region of rectangular channels usually neglect the free convection effects [1–3]. However, recently it has been shown that the free convection effects can be quite significant in the thermal entrance region and as a matter of fact the classical Graetz problem represents

only a limiting case [4]. A survey of the literature reveals that a theoretical analysis on thermal entrance region problem (Graetz problem) in horizontal ducts taking free convection effects into consideration is non-existent for the case of uniform wall temperature condition. For heating of fluids flowing in horizontal ducts, the buoyant forces cause a circulation upward at the sides and downward at the center of the duct. The combined effects of secondary flow and the forced main flow then set up the forward moving spirals. The consequent mixing due to secondary flow is known to increase the heat-transfer coefficient.

In contrast to the case of uniform wall heat flux boundary condition, the free convection effect is expected to be insignificant for the case of uniform wall temperature condition as the thermally fully developed region is approached. Experimental investigations on heat transfer due to combined free and forced convection in the thermal entrance region of horizontal tubes with isothermal wall have been reported and the empirical correlation equations have been proposed by several investigators [5–7]. However, the empirical correlation equations for heat transfer are extremely difficult to develop because of the rather large scatter of the experimental data and the lack of basic understanding on heat-transfer mechanism involving secondary flow in the thermal entrance. Furthermore, in the case of rectangular channels the empirical correlation is expected to be complicated by the multiplicity of parameters involved.

The difficulty of obtaining theoretical solution for thermal entrance region problem with buoyancy effects was pointed out in [4]. However, for large Prandtl number fluids the problem can be approached by noting that the inertia terms in the axial momentum and vorticity transport equations can be neglected. As a result the primary flow becomes independent of the secondary flow but the convection terms due to secondary flow in the energy equation must be retained.

The purpose of this paper is to study the buoyancy effects on thermal entrance region heat transfer in horizontal rectangular channels having aspect ratios (horizontal width/vertical height) 0·5, 1 and 2 with uniform wall temperature for large Prandtl number fluids. The study was made in an attempt to clarify the local Nusselt number behavior in the thermal entrance region in general and the onset of significant free convection effects and the subsequent asymptotic behavior in particular. The numerical results obtained may also provide some guide in future experimental investigations.

2. GOVERNING EQUATIONS

Consider a steady fully-developed laminar flow of a viscous fluid in a horizontal rectangular channel where

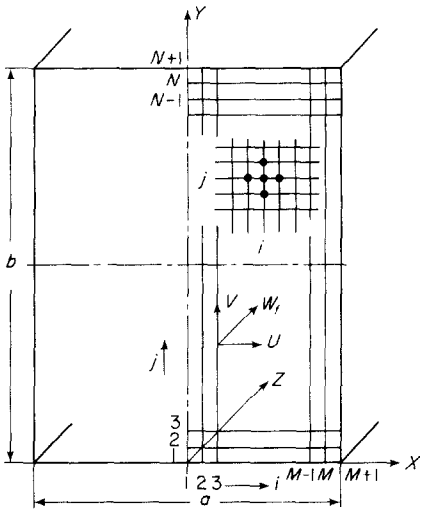

FIG. 1. Coordinate system and numerical grid for a horizontal rectangular channel.

a step change in wall temperature is imposed at the entrance Z = 0 (see Fig. 1). The problem is to find the temperature development and the related heat-transfer coefficient along the heated or cooled section of the channel. The formulation of the problem considering the free convection effects based on Boussinesq approximation and neglecting the axial conduction effect is presented in [4]. The governing equations valid for large Prandtl number fluids are then reduced from the general formulation [4]. Referring to the co-ordinate system shown in Fig. 1 and introducing the following dimensionless variables and parameters,

$$X = [D_e]x, \quad Y = [D_e]y, \quad Z = [D_e PrRe]z,$$
$$U = [\kappa/D_e]u, \quad V = [\kappa/D_e]v, \quad W_f = [\overline{W}_f]w_f,$$
$$P_f = [P_c]P_f, \quad T - T_w = [\theta_c]\theta, \quad Gr = g\beta\theta_c D_e^3/\nu^2,$$
$$Pr = \nu/\kappa, \quad Ra = PrGr, \quad Re = \overline{W}_f D_e/\nu$$

where $D_e = 4A/S$ and $\theta_c = T_0 - T_w$, the following governing equations for the large Prandtl number case can be obtained [4].

Axial momentum equation

$$\nabla^2 w_f = C. \tag{1}$$

Vorticity transport equation

$$\nabla^2 \xi = Ra \frac{\partial \theta}{\partial x}. \tag{2}$$

Stream function equation

$$\nabla^2 \psi = \xi. \tag{3}$$

Energy equation

$$\nabla^2 \theta = \frac{\partial}{\partial x}(u\theta) + \frac{\partial}{\partial y}(v\theta) + w_f \frac{\partial \theta}{\partial z}. \tag{4}$$

where

$$\nabla^2 = \partial^2/\partial x^2 + \partial^2/\partial y^2,\ C = (D_e^2/\mu \bar{W}_f)\partial P_f/\partial Z = \text{constant}$$
$$u = \partial\psi/\partial y \quad \text{and} \quad v = -\partial\psi/\partial x.$$

It is noted that the inertia terms in the axial momentum and vorticity transport equations have been neglected because of large Prandtl number assumption [4]. The equations (1)–(3) are of elliptic type and the energy equation (4) which is in a conservation form [8] is of parabolic type. The equations (2)–(4) are coupled but the free-convective effect is seen to be linearly superimposed upon the forced convection. The boundary conditions are:

$$\begin{aligned} u = v = w_f = \psi = \theta = 0 \quad &\text{at wall} \\ \theta = 1 \quad &\text{at entrance } z = 0. \end{aligned} \tag{5}$$

In addition, $\xi = \psi = 0$ along the vertical center line from the assumption of symmetry depending upon the stability of the flow and the boundary vorticity for equation (2) is unknown. The present formulation is based on cooling of the fluid ($T_0 > T_w$). However, the results are applicable also to the heating case ($T_w > T_0$). This is evident when one considers the basic equations for the case ($T_w > T_0$).

In the present formulation valid for large Prandtl number the forced flow (on its own) is always considered to be, hydrodynamically fully developed Poiseuille type flow. Furthermore, the order of magnitude analysis [4] reveals that the buoyant-flow development is significant and must be taken into account. The forced flow development was not considered in the analysis because of mathematical difficulty. It should be emphasized that, the present formulation is based upon a linearization of the equations of motion.

The analytical solution of the problem is apparently not practical and a numerical approach will be used. After obtaining the developing temperature field, the computation of the local Nusselt number is of practical interest. The Nusselt number $Nu = \bar{h}D_e/k$ may be obtained by considering the temperature gradient at the wall or the overall energy balance for the axial length dZ as,

$$\begin{aligned} Nu_1 &= -(\overline{w_f \partial\theta/\partial z})/4\theta_b \\ Nu_2 &= -(\overline{\partial\theta/\partial n})/\theta_b \end{aligned} \tag{6}$$

where

$$\theta_b = \int_A w_f \theta \, dA \Big/ \int_A w_f \, dA.$$

3. FINITE-DIFFERENCE SOLUTION

The details regarding the finite-difference equations are omitted here. The exact analytical solution of the Poisson's equation (1) is available and the accurate axial velocity field can be computed by using the first ten terms of the series solution [3,9]. Briefly, the known computational procedure for the simultaneous solution of the remaining equations (2)–(4) consists of the following main steps for a given value of Rayleigh number:

1. The numerical solution starts with equation (4) using the alternating direction implicit (ADI) method [10].
2. Equation (2) is then solved by using the line iterative method [10] where the boundary vorticity of the previous section is used to compute the current interior vorticity.
3. The stream function ψ is obtained by solving equation (3) using line iterative method [10]. The boundary vorticity is obtained by first reducing equation (3) at boundary and then approximating the derivatives by second order correct finite-difference equation [8].
4. The secondary velocity components u, v are computed from the known stream function.
5. The axial step is advanced by one and steps 1 to 4 are repeated.

Usually at each axial step, the iterations of equations (2) and (3) are carried out until the vorticity and the stream function satisfy the preassigned convergence criterion. However, numerical stability for the parabolic equation (4) particularly near the thermal entrance leads to a restriction on the axial step size and the iteration procedure is found to be impractical for the present entrance region problem. After considerable numerical experiment the axial step sizes Δz varying from 10^{-7} near the entrance to 5×10^{-4} near the fully developed region are found to be satisfactory. This results in approximately 1515 axial steps. For steps 2 and 3, two calculations are performed; the first one starts at the bottom line $j = 1$ (see Fig. 1) and ends at the top line $j = N+1$ with the second one in the opposite direction.

The cross-sectional mesh size at each axial section is determined by studying the convergence of the limiting case $Ra = 0$ particularly near the entrance $z = 0$. The discussion on the convergence of the numerical results will be made in next section. Accurate numerical solution is required near the entrance since at higher values of Rayleigh number the onset of significant secondary flow effect appears early. The mesh sizes ($M \times N$) of 16×32, 12×48 and 24×24 are finally used for the aspect ratios $\gamma = 1$, 0·5 and 2 respectively. The required computing time for each axial step is approximately 0·8 s on IBM 360/67. Noting that $Ra = PrGr$, the present formulation is seen to be valid for any large Ra. However, the numerical difficulty arises when $Ra > 5 \times 10^5$.

4. HEAT-TRANSFER RESULTS

The temperature profile development is of interest in understanding the local Nusselt number behavior in the thermal entrance region and the example cases of $Ra = 10^5$, $\gamma = 1$ and $Ra = 2 \times 10^5$, $\gamma = 2$ are shown in Figs. 2 and 3, respectively. It is seen that for square channel $\gamma = 1$ the normal temperature gradients at the upper wall are greater than those at the lower wall and the maximum value for θ is located near the upper wall. The axial bulk temperature distributions θ_b for the aspect ratios $\gamma = 1$, 2 and 0·5 are shown in Figs. 4–6, respectively, for several values of Rayleigh number. The local Nusselt number variations with Rayleigh number as parameter are shown in Figs. 7–9 for the aspect ratios $\gamma = 1$, 2 and 0·5, respectively.

The local Nusselt number variations shown in Fig. 7 for horizontal square channel $\gamma = 1$ reveal that the onset of secondary flow effect due to buoyancy forces occurs at a certain entrance distance depending on the value of Rayleigh number. Up to the onset point, the Graetz theory applies. In this respect, the onset of secondary flow effect is of practical interest in design and the correlation equations for the prediction of

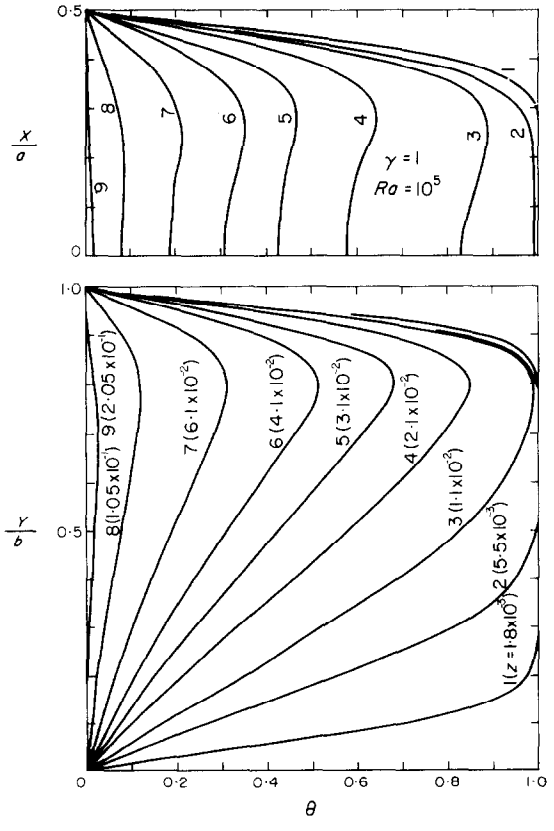

FIG. 2. Developing temperature profiles along horizontal and vertical center lines for $\gamma = 1$ and $Ra = 10^5$.

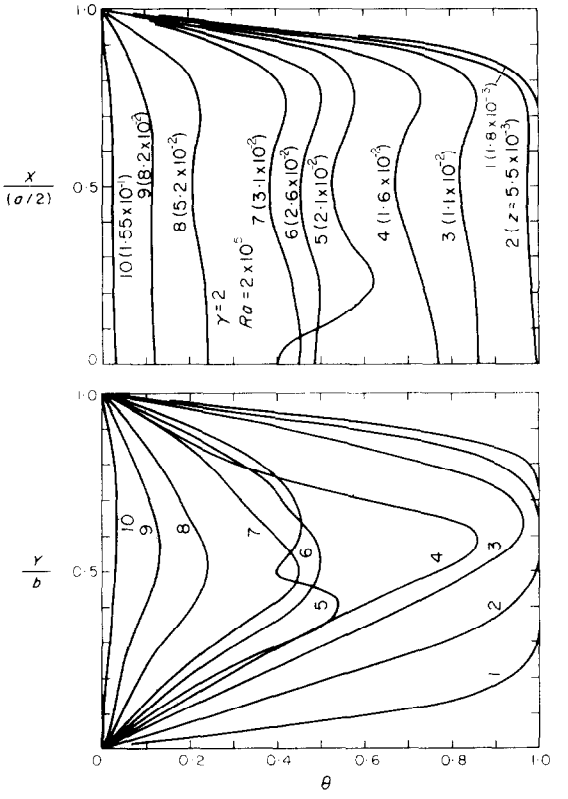

FIG. 3. Developing temperature profiles along horizontal and vertical center lines for $\gamma = 2$ and $Ra = 2 \times 10^5$.

the onset point based on 2 per cent deviation of local Nusselt number from that of the Graetz theory ($Ra = 0$) are developed for the aspect ratios $\gamma = 1$, 2 and 0·5 and the results together with the data points are shown in Fig. 10. As shown in Fig. 7 for $Ra = 10^3$ the free convection effect is practically insignificant and the maximum deviation of the Nusselt number from Graetz theory ($Ra = 0$) is found to be only 0·8 per cent. This fact clearly demonstrates that the Graetz theory is a limiting case and applicable only when $Ra \leqslant 10^3$. Some insight regarding the local Nusselt number behavior may be gained by contrasting the temperature profile developments, for example, for θ and θ_b shown in Figs. 2 and 4, respectively, with Nusselt number variation shown in Fig. 7 for $\gamma = 1$ and $Ra = 10^5$. The decrease of Nusselt number in thermal entrance region for Graetz problem ($Ra = 0$) is known to be the entrance effect due to axial convective term only and the deviation from Graetz theory represents the increase of Nusselt number over Graetz theory due to free convection effect. It is clear that the entrance and free convection effects will eventually balance out and the local minimum Nusselt number appears at some downstream location depending on the value of Rayleigh number. Subsequently, the

free convection effect dominates over the entrance effect and the Nusselt number increases until the local maximum value for Nu is reached. For the present uniform wall temperature condition the temperature difference $\Delta T = T_b - T_w$ giving rise to free convection proached from above. The physical mechanism for heat transfer is now clear. One may further note that the developing temperature profiles 2 and 4 shown in Fig. 2 correspond to the local minimum and maximum Nusselt number points, respectively, for $Ra = 10^5$

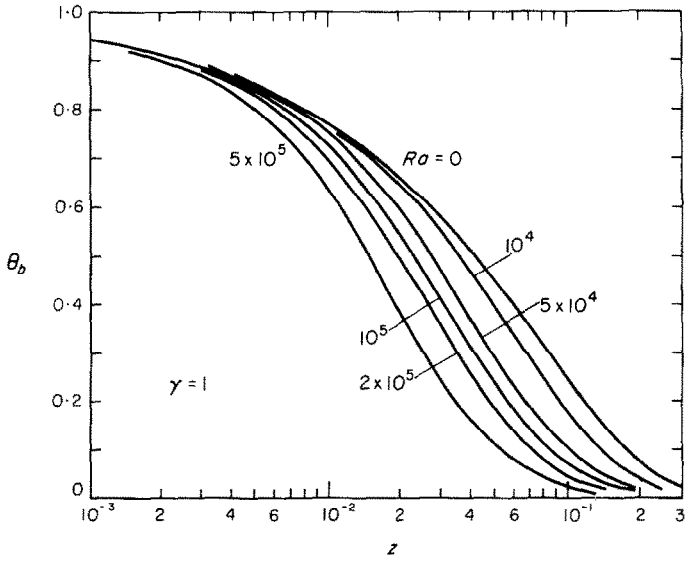

FIG. 4. Axial bulk temperature distribution for $\gamma = 1$ with Ra as parameter.

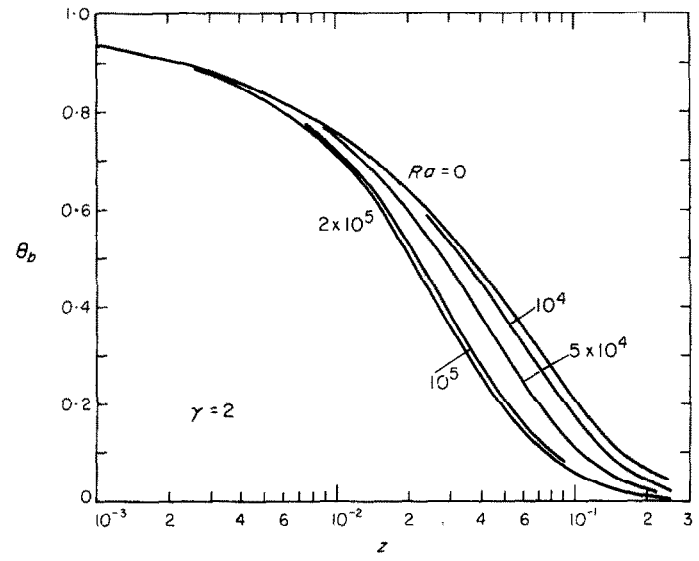

FIG. 5. Axial bulk temperature distribution for $\gamma = 2$ with Ra as parameter.

effect gradually decreases as the asymptotic condition is approached ($\theta_b \to 0$). It is then clear that after reaching the local maximum value for Nu, the local Nusselt number decreases again due to entrance effect until the theoretical Graetz curve ($Ra = 0$) is approached from above. The physical mechanism for heat transfer is now clear. One may further note that the developing temperature profiles 2 and 4 shown in Fig. 2 correspond to the local minimum and maximum Nusselt number points, respectively, for $Ra = 10^5$ shown in Fig. 7. At the location with minimum Nusselt number, the central core with uniform entrance temperature T_0 disappears completely.

The Nusselt number behavior for the other aspect ratios $\gamma = 2$ and 0·5 is qualitatively similar to that of

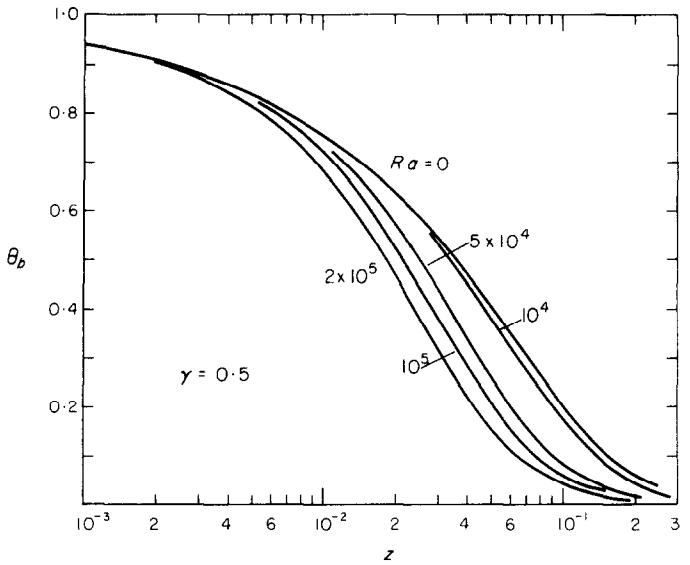

FIG. 6. Axial bulk temperature distribution for $\gamma = 0{\cdot}5$ with Ra as parameter.

$\gamma = 1$. However, at $Ra = 5 \times 10^5$ for $\gamma = 1$ and $Ra = 2 \times 10^5$ for $\gamma = 2$ the increase of the Nusselt number after reaching the local minimum Nusselt number point and the decrease of the Nusselt number subsequent to attaining the local maximum value are both seen to be rather rapid. An examination of the secondary flow patterns reveals that within the range $z = 8 \times 10^{-3} \sim 7 \times 10^{-2}$ for $\gamma = 1$, $Ra = 5 \times 10^5$ and $z = 10^{-2} \sim 10^{-1}$ for $\gamma = 2$, $Ra = 2 \times 10^5$, four vortices for secondary flow appear. Similar situation also occurs for the range $z = 1{\cdot}6 \times 10^{-2} \sim 6 \times 10^{-2}$ with $Ra = 2 \times 10^5$, $\gamma = 1$ and $z = 1{\cdot}6 \times 10^{-2} \sim 2{\cdot}6 \times 10^{-2}$ with $Ra = 10^5$, $\gamma = 2$.

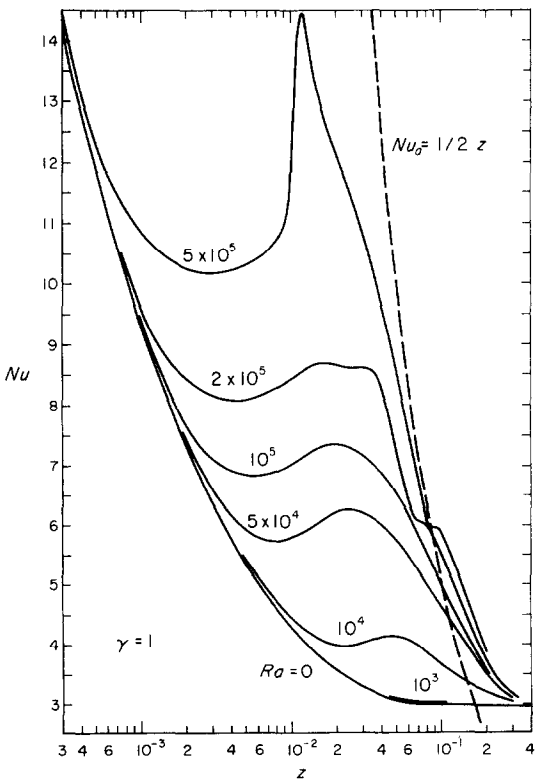

FIG. 7. Local Nusselt number variation for $\gamma = 1$ with Ra as parameter.

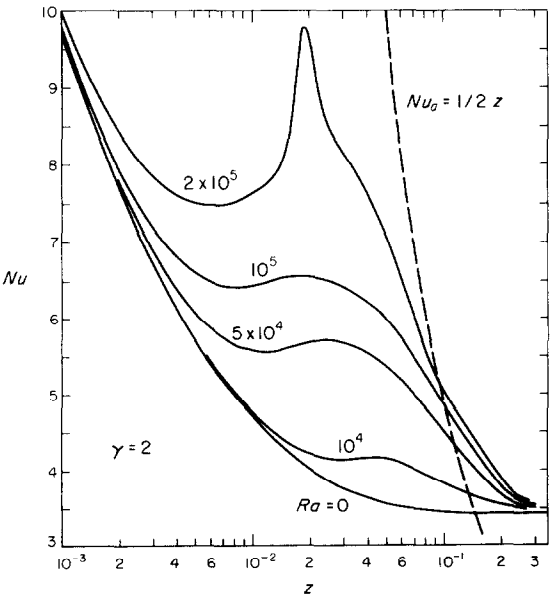

FIG. 8. Local Nusselt number variation for $\gamma = 2$ with Ra as parameter.

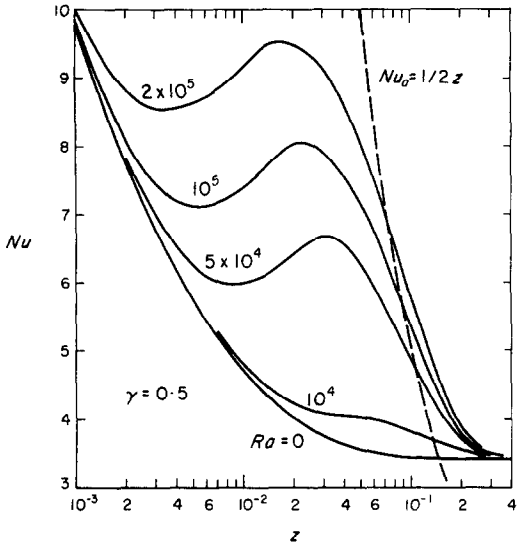

FIG. 9. Local Nusselt number variation for $\gamma = 0.5$ with Ra as parameter.

The typical secondary flow field illustrating the direction of the secondary velocity vector only is shown in Fig. 11 for $\gamma = 2$ and $Ra = 2 \times 10^5$ at $z = 2.1 \times 10^{-2}$. For the case of heating at the wall, the secondary flow pattern becomes the mirror image of that shown in Fig. 11. The fluid moves upward near the side wall and toward the vertical center line along the upper wall with the corresponding shift for the centers of vortex rolls. When four vortex rolls appear, the values of the boundary vorticities are found to change the sign. As a result, the developing temperature profile is also varied and the typical profiles are shown as curves 5 in Fig. 3 for $\gamma = 2$ and $Ra = 2 \times 10^5$. The particular temperature profiles can be understood readily when one notes the secondary flow pattern shown in Fig. 11. It is to be noted that for the aspect ratio $\gamma = 0.5$ where the vertical height of the channel is twice the horizontal width, the above mentioned secondary flow pattern is not observed even at $Ra = 2 \times 10^5$. The present numerical solution shows that four vortex rolls may appear at higher Rayleigh numbers for horizontally wide rectangular channels with $\gamma \geqslant 1$.

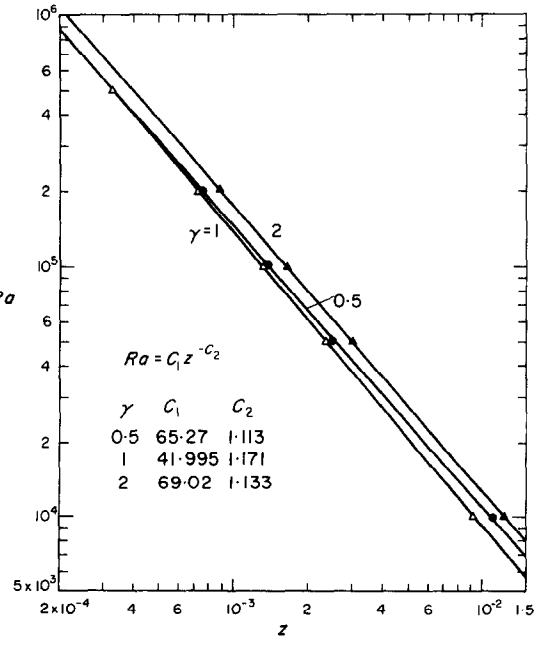

FIG. 10. Correlation equation for the onset of free convection effect based on 2 per cent deviation of local Nusselt number from that of classical Graetz theory ($Ra = 0$).

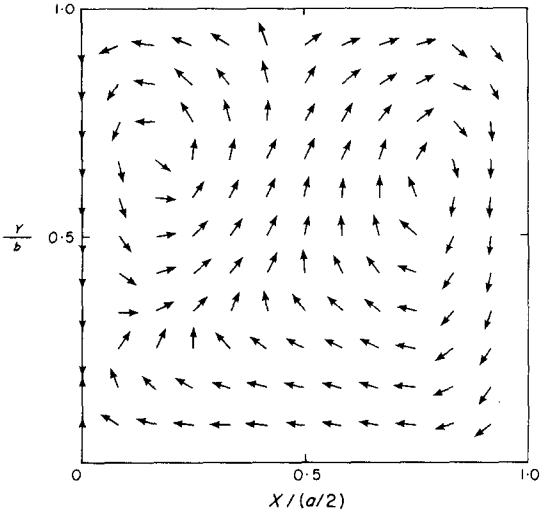

FIG. 11. Secondary flow pattern showing the direction of secondary velocity vectors for $\gamma = 2$ and $Ra = 2 \times 10^5$ at $z = 2.1 \times 10^{-2}$.

For Graetz problem in circular tubes with uniform wall temperature, the asymptote for the Nusselt number based on the arithmetic mean temperature difference $(T_0 - T_w)/2$ representing the condition that the outflowing liquid has reached the tube wall temperature T_w is reported by McAdams [11] and can be readily applied to the present rectangular channel problem as $Nu_a \equiv h_a D_e/k = 1/2z$. For the present thermal entrance region problem in horizontal rectangular channels with uniform wall temperature the asymptote Nu_a is of special interest and is shown in Figs. 7–9 for reference. Although the asymptote Nu_a is based on the average heat-transfer coefficient h_a over the entrance length and arithmetic mean temperature difference [11], it is nevertheless instructive in understanding the asymptotic behavior of the local Nusselt number for the present study.

At this point, it is appropriate to discuss the accuracy and convergence of the numerical results. For the range of entrance region where the free convection effect is significant, the convergence criterion [4],

$$\varepsilon = \sum_{i,j} |f_{i,j}^{(n+1)} - f_{i,j}^{(n)}| / \sum_{i,j} |f_{i,j}^{(n+1)}| < 4 \times 10^{-3},$$

is generally satisfied for ψ, ξ and θ except at higher values of Rayleigh number. For $Ra = 5 \times 10^5$, $\gamma = 1$ and $Ra = 2 \times 10^5$, $\gamma = 2$, the error ε as defined above reaches as high as $1{\cdot}8 \times 10^{-2}$ at several downstream sections near the peak of the local Nusselt number. As noted in Section 2, the local Nusselt number can be computed in two ways. The numerical results for Nu_2 based on average normal temperature gradient at wall are expected to have relatively higher error since the temperature gradient is greater near the wall and a smaller mesh size is required to evaluate the wall temperature gradient accurately. With sufficiently small axial steps such as those finally used in the present study, it is then clear that the Nusselt number Nu_1 based on overall energy balance gives more accurate results. It is found that the two Nusselt numbers, Nu_1 and Nu_2 generally agree well for the region between the onset of secondary flow effect and fully developed condition. For example, for $Ra \leqslant 5 \times 10^4$ with $\gamma = 1$ and 0·5 and $Ra \leqslant 10^5$ with $\gamma = 2$, the deviation of Nu_2 from Nu_1 is less than 1 per cent. At higher values of Rayleigh number, the maximum deviation of approximately 4 per cent occurs at $z \approx 10^{-3}$ but the deviation elsewhere is still generally less than 1 per cent. The maximum deviation is believed to be caused by inaccurate evaluation of local wall temperature gradient $\partial\theta/\partial n$. The numerical results presented for Nu are based on Nu_1 and are believed to be accurate within 1 per cent. The asymptotic Nusselt numbers of 2·988 for $\gamma = 1$ and 3·3946 for $\gamma = 2$, obtained in this study agree excellently with the known results [12].

5. CONCLUDING REMARKS

1. For the range of Rayleigh numbers $0 \sim 5 \times 10^5$ and aspect ratios $\gamma = 0{\cdot}5$, 1, 2 investigated, the free convection effect on laminar heat transfer in the thermal entrance region of horizontal rectangular channels with uniform wall temperature is found to be significant only in some entrance region depending on aspect ratio (see Figs. 7–9). It is worth noting that the free convection effect is negligible near the thermal entrance and in the thermally fully developed region. Also the free convection effect is practically negligible only when $Ra \leqslant 10^3$.

2. The two limiting (asymptotic) cases for the present analysis are of interest. When $Ra/Re \to 0$, one obtains the classical Graetz problem. When $Ra/Re \to \infty$ or $W_f \to 0$, the problem reduces to natural convection in a rectangular cavity. In this connection the references [13, 14] should be mentioned.

3. In view of the considerable difficulty in obtaining theoretical solution without large Prandtl number assumption, the practical question arises as to whether or not the present results can be applied to Prandtl number, say, 10. In the absence of theoretical analysis valid for any Prandtl number, the question can be answered only by comparison with experimental results. In this connection, some experimental results which appear to indicate the free convection effect are shown in Fig. 6 of [3] but apparently the experiment was not designed to study the effect. In the absence of further detailed information, a comparison with the present result is not made here.

4. The present numerical results clearly suggest the difficulty in obtaining an empirical correlation equation for heat transfer valid for a range of Prandtl numbers using the experimental data [5–7].

5. The circumstances under which the four vortices may appear need further investigation. When the vertical height of the horizontal rectangular channel is greater than the horizontal width, $b > a$, the appearance of the four vortices is probably not likely because of side wall effect. On the other hand, when $b \leqslant a$ the four vortices may appear at higher Rayleigh number. From the viewpoint of thermal instability, the vertical center line temperature profiles shown in Fig. 3 for $\gamma = 2$ reveal that only the upper half of the channel cross-section is unstable for the cooling case under consideration and this observation seems to be confirmed by the secondary flow pattern shown in Fig. 11.

6. The asymptotic behavior of local Nusselt number for the present problem is of special interest. For the aspect ratios and Rayleigh numbers under consideration, the free convection effect can be neglected practically at approximately $z = 5 \times 10^{-1}$.

Acknowledgement—This work was supported by the National Research Council of Canada and the Petroleum Education Aid Fund of Alberta through operating and computing grants. The referees provided valuable comments leading to improvement in the presentation.

REFERENCES

1. S. C. R. Dennis, A. McD. Mercer and G. Poots, Forced heat convection in laminar flow through rectangular ducts, *Q. Appl. Math.* **17**, 285–297 (1959).
2. E. M. Sparrow and R. Siegel, Application of variational methods to the thermal entrance region of ducts, *Int. J. Heat Mass Transfer* **1**, 161–172 (1960).
3. S. R. Montgomery and P. Wibulswas, Laminar flow heat-transfer in ducts of rectangular cross-section, *Procs. Third International Heat Transfer Conference*, Vol. 1, pp. 104–112. A.I.Ch.E., New York (1966).
4. K. C. Cheng, S. W. Hong and G. J. Hwang, Buoyancy effects on laminar heat transfer in the thermal entrance

region of horizontal rectangular channels with uniform wall heat flux for large Prandtl number fluid, *Int. J. Heat Mass Transfer* **15**, 1819–1836 (1972).
5. D. R. Oliver, The effect of natural convection on viscous-flow heat transfer in horizontal tubes, *Chem. Engng Sci.* **17**, 335–350 (1962).
6. A. R. Brown and M. A. Thomas, Combined free and forced convection heat transfer for laminar flow in horizontal tubes, *J. Mech. Engng Sci.* **7**, 440–448 (1965).
7. C. A. Depew and S. E. August, Heat transfer due to combined free and forced convection in a horizontal and isothermal tube, *J. Heat Transfer* **93**, 380–384 (1971).
8. K. E. Torrance, Comparison of finite-difference computations of natural convection, *J. Res. Natn. Bur. Stand.* **72B**, 281–301 (1968).
9. J. G. Knudsen and D. L. Katz, *Fluid Dynamics and Heat Transfer*, p. 101. McGraw-Hill, New York (1958).
10. D. Young, The numerical solution of elliptic and parabolic partial differential equations, in *Survey of Numerical Analysis*, edited by J. Todd, pp. 380–438. McGraw-Hill, New York (1962).
11. W. H. McAdams, *Heat Transmission*, p. 232. McGraw-Hill, New York (1954).
12. W. M. Rohsenow and J. P. Hartnett (Editors), *Handbook of Heat Transfer*, pp. 7–119. McGraw-Hill, New York (1973).
13. S. H. Clark and W. M. Kays, Laminar-flow forced convection in rectangular tubes, *Trans. Am. Soc. Mech. Engrs* **74**, 859–866 (1953).
14. G. De Vahl Davis, Laminar natural convection in an enclosed rectangular cavity, *Int. J. Heat Mass Transfer* **11**, 1675–1693 (1968).

EFFET DE LA CONVECTION NATURELLE DANS LE PROBLEME DE GRAETZ POUR DES CANAUX RECTANGULAIRES HORIZONTAUX AVEC TEMPERATURE PARIETALE UNIFORME ET POUR DES GRANDS *Pr*

Résumé—On étudie par une méthode numérique l'effet d'Archimède sur la convection thermique laminaire et forcée dans la région d'entrée de canaux rectangulaires horizontaux avec une température pariétale uniforme, dans le cas des nombres de Prandtl élevés. On présente les résultats numériques pour des rapports largeur/hauteur égaux à 0,5–1–2 et des nombres de Rayleigh compris entre zéro et 5×10^5. On établit les équations de corrélation pour le début de l'effet sensible de la convection naturelle. Le comportement asymptotique du nombre de Nusselt local est comparé avec l'asymptote connue pour la condition de température pariétale uniforme. On délimite clairement les conditions où l'effet de la convection naturelle est significatif, et le problème classique de Graetz est un cas limite applicable seulement quand $Ra \leqslant 10^3$.

EINFLUSS DER FREIEN KONVEKTION BEIM GRÄTZ-PROBLEM IN HORIZONTALEN RECHTWINKLIGEN KANÄLEN MIT EINHEITLICHER WANDTEMPERATUR BEI GROSSEN PRANDTL-ZAHLEN

Zusammenfassung—Beim Wärmeübergang bei erzwungener Konvektion mit laminarer Strömung in der thermischen Anlaufstrecke von horizontalen rechtwinkligen Kanälen mit gleichförmiger Wandtemperatur wird für den Fall von Fluiden mit großer Prandtl-Zahl mittels einer numerischen Methode der Einfluß der Auftriebskräfte untersucht.

Die numerischen Lösungen werden für das Seitenverhältnis (Breite/Höhe) 0,5, 1, 2 und Rayleigh-Zahlen von $0–5.10^5$ dargestellt. Die Korrelationsgleichungen zur Bestimmung des Beginns des Einflusses der freien Konvektion werden entwickelt. Das asymptotische Verhalten der Nusselt-Zahl wird verglichen mit der bekannten Asymptote für die Randbedingung der gleichförmigen Wandtemperatur. Die Einlaufstrecke, in der der Einfluß der freien Konvektion von Bedeutung ist, wird klar nachgewiesen, und es wird gezeigt, daß das klassische Grätz-Problem ein Grenzfall ist und nur anwendbar für $Ra \leqslant 10^3$.

ВЛИЯНИЕ ЕСТЕСТВЕННОЙ КОНВЕКЦИИ В ЗАДАЧЕ ГРЭТЦА ДЛЯ ГОРИЗОНТАЛЬНЫХ КАНАЛОВ ПРЯМОУГОЛЬНОГО СЕЧЕНИЯ С ПОСТОЯННОЙ ТЕМПЕРАТУРОЙ СТЕНКИ ПРИ БОЛЬШИХ ЧИСЛАХ ПРАНДТЛЯ

Аннотация — Проведено численное исследование влияния выталкивающих сил на теплообмен в ламинарном течении при вынужденной конвекции на тепловом входном участке в горизонтальных каналах с постоянной температурой стенки прямоугольного сечения для жидкостей с большим числом Прандтля. Приводятся численные результаты, полученные при отношениях сторон (ширины к высоте) 0,5; 1; 2 и числах Релея $0 \sim 5 \times 10^5$. Построены корреляционные уравнения для определения возникновения значительного влияния свободной конвекции. Проведено сравнение асимптотического поведения локального числа Нуссельта с известным значением для каналов с постоянной температурой стенки. Точно определен входной участок, где влияние свободной конвекции весьма существенно, и показано, что классическая задача Грэтца является предельным случаем и справедлива только при $Ra \leq 10^3$.